Best Dioctahedral Smectite for Nitrogen Heterocyclics Adsorption−A Reactivity Index Study

Abhijit Chatterjee,* Takeo Ebina, and Takashi Iwasaki

National Institute of Advanced Industrial Science and Technology, AIST Tohoku, 4-2-1 Nigatake, Miyagino-ku, Sendai 983-8551, Japan

Received: February 16, 2001; In Final Form: August 28, 2001

The activity of nitrogen heterocyclics present in biomacromolecules and its suitable sorbent from the dioctahedral smectite family is investigated using a range of reactivity index using density functional theory (DFT). For the first time, a novel function λ has been defined for quantitative description of weak adsorption cases, which was so far qualitative inside the domain of DFT. From the values of the local softness, it is concluded that the local acidities of the inorganic material systems are dependent on several characteristics, which are of importance within the framework of the hard and soft acids and bases (HSAB) principle. We first rationalized an understanding of the electronic structures of a range of nitrogen heterocyclics ranging from indole, imidazole, pyrrole, and pyridine, followed by the local softness calculation to locate its active site. We compared its activity with that of the OH group of isomorphously substituted (Fe^{3+}, Mg^{2+}, Fe^{2+}, and Li^{+}) dioctahedral smectite family. Two types of interactions were identified between heterocyclics and smectite. The ordering for best sorption follows the order $Mg^{2+} > Fe^{2+} > Fe^{3+} > Li^{+}$, whereas the order for best sorbent is imidazole > pyridine > pyrrole > indole. The results rationalize the experimental observation.

Introduction

Cation−π interactions are becoming an important and general noncovalent binding force.[1] Extensive experimental and theoretical efforts have been made in the past decade to monitor the role of cation−π interactions in biological science.[2−8] It has been shown that cations can bind strongly to the π face of an aromatic system. Cation−π interaction is much stronger than hydrogen bond and hydrophobic interactions. Hence, there is a prime need for a better understanding of the cation−π interaction, which might help us in designing new catalysts, drugs, proteins, and enzymes. Now, it is observed that exchangeable cations on clays strongly influence their sorptive characteristics for organic compounds especially nonionic in nature.[9] The net negative charge on dioctahedral smectite layers has been generated by the substitution of an octahedral/tetrahedral cation. The resulting negative charge is then counter balanced by interlayer exchangeable cation. The hydration of these exchangeable cations and the Si−O groups in clay surfaces are responsible for the hydrophilic nature of the clay surface. As a result, nonionic organic compounds adsorption is suppressed in the presence of water because relatively nonpolar organic compounds cannot effectively compete with highly polar water for adsorption sites on the clay surface. In the absence of water, the clay surface acts as a solid adsorbent.[10,11] Biomacromolecules are too big to be investigated using high-level theoretical modules. Benzene could be the right choice in terms of symmetry but the complexity of biomolecules cannot be depicted truly by benzene. At the same time, biomolecules are constituted with nitrogen heterocyclics, so the use of the latter best suits the purpose. Hence, we choose nitrogen heterocyclics as the interacting molecule. We wish to find an appropriate adsorbent which is cheap and easily available and has a cation to interact with the heterocyclics. Preconcentration is a very useful phenomenon to be performed for a molecular interaction where the concentrations of the interacting molecules are less. This study also foresees the utility of such an adsorbent inorganic material to be useful in adsorbing toxic organic components. We want to explore the isomorphously substituted smectites to probe their activity toward nitrogen heterocyclics and will propose a novel scale for choosing the particular clay without tedious experimentation. Bailey et al.[12] have shown that monoclinic dioctahedral mica has two independent types of octahedra. The two OH groups of each octahedra lie on the symmetry plane of each layer; for the first octahedra it lies in the trans orientation, and in the second case, it lies at the cis position. Now in the case of the smectites, the activity solely lies on the orientation of the hydroxyl hydrogen attached to the octahedral aluminum present in 2:1 dioctahedral smectite. Sposito et al.[13] pointed out that in case of dioctahedral clays the OH bond is directed parallel to the clay sheet with the hydrogen pointing to the octahedral vacancy. This OH may act as the active site for molecular adsorption, as proposed by Delville et al.[14] They have modeled the clay−water interactions. They have shown that the water molecules form a hydrogen bond with the lone pair of the oxygen at the center of the hexagonal cavity. This is possible for dioctahedral clays, because the proton is directed parallel to the plane of the clay. There are suggestions from electrostatic calculations[15] that the orientations of these hydroxyl groups are sensitive to the octahedral cation plane at the center of the clay layer. Because these hydroxyl groups may be expected to play a major role in the

* To whom correspondence should be addressed. E-mail: c-abhijit@aist.go.jp. Phone: +81-22-237-5211. Fax: +81-22-237-5217.

10.1021/jp010626r CCC: $20.00
Published on Web 11/07/2001

catalytic activity of 2:1 clays, it is important to examine their orientation more closely. We therefore want to explore the role of this hydroxyl hydrogen with isomorphous substitution and will probe the stability of the adsorption complex of nitrogen heterocyclics with the smectite surface. We want to emphasize the interaction between the active site of the dioctahedral clay, which is the hydroxyl group present in the octahedral layer of the clay, and the active site of nitrogen heterocyclic molecules.

So far, there are many experimental and theoretical studies to monitor the interaction of molecules with the clay surface, but there is no effort so far to correlate the activity of the molecules in terms of interaction with the clay surface. Now, the hard−soft acid−base (HSAB) principles classify the interaction between acids and bases in terms of global softness. Pearson proposed the global HSAB principle.[16] The global hardness was defined as the second derivative of energy with respect to the number of electrons at constant temperature and external potential, which includes the nuclear field. The global softness is the inverse of this. Pearson also suggested a principle of maximum hardness (PMH),[17] which states that, for a constant external potential, the system with the maximum global hardness is most stable. In recent days, DFT has gained widespread use in quantum chemistry. Some DFT-based local properties, e.g., Fukui functions and local softness,[18] have already been used for the reliable predictions in various types of electrophilic and nucleophilic reactions.[19−22] In our recent study,[23a] we proposed a reactivity index scale for heteroatomic interaction with zeolite framework. Moreover, Gazquez and Mendez[24] proposed that when two molecules A and B of equal softness interact, thereby implicitly assuming one of the species as nucleophile and the other as an electrophile, then a novel bond would likely form between an atom A and an atom B whose Fukui function values are close to each other. Now earlier we have seen that the local descriptors behave nicely for unidenate interaction;[23a] that is, when the active atom of the interacting molecule is remarkably electrophilic in comparison to other atoms of the molecule, then it undergoes a favorable interaction with the most nucleophilic site of the framework cluster. This is very sensitive with a situation with monodentate interaction and a bidentate interaction, i.e., a situation when two of the atoms of the molecule are having comparable activities. This situation is elaborated in our recent papers.[25−27] Now Pal et al.[28] recently proposed that reactivity descriptors can be used to predict the weak interactions in a quantitative way. They defined a parameter λ, which bears information about the stability of the system. Their study is related with very small gaseous molecules. We therefore tried their approach to find the applicability of the proposition in deriving the interaction energy correlations to generate a quantitative scale to chose a best sorbent for a particular molecular interaction; here, it is nitrogen heterocyclics.

In the present study, we first use DFT-based local reactivity descriptors to correlate the activity of the nitrogen heterocyclics with different isomorphously substituted (Fe^{3+}, Mg^{2+}, Fe^{2+}, and Li^{+}) dioctahedral smectite surfaces. A cluster model was generated from the crystal structure of dioctahedral smectite montmorillonite, which is considered to reproduce and compare the effect of the environment on the activity of the active center present in the clay surface. The reactivity indexes of nucleophilic and electrophilic sites were compared. An activity order is proposed. The results were compared with the interaction energy calculations with each of the isomorphously substituted clay cluster using DFT. While discussing the absolute activity of the clay surface and the energy associated with each isomorphous substituted product, the focus has been kept on evaluation and comparison of the λ parameter and its effect on the adsorption energy. A scale of activity is proposed in terms of the reactivity index, which paves a novel way of designing new material for a particular reaction of environmental importance. This new parameter, λ, at the same time can successfully identifies the different type of interactions, viz., (1) hydrogen bonding type and (2) cation-π type, taking place with nitrogen heterocyclics and clay structure.

Theory

Let us first recall the definition of various quantities employed. The Fukui function $f(r)$ is defined by[18]

$$f(r) = [\delta\mu/\mathrm{d}v(r)]_N = [\delta\rho(r)/\delta N]_v \quad (1)$$

The function f is thus a local quantity, which has different values at different points in the species, and N is the total number of electrons. Because $\rho(r)$ as a function of N has slope discontinuities, eq 1 provides the following three reaction indices:[18]

$$f^{-}(r) = [\delta\rho(r)/\delta N]_v^{-} \quad \text{(governing electrophilic attack)}$$

$$f^{+}(r) = [\delta\rho(r)/\delta N]_v^{+} \quad \text{(governing nucleophilic attack)}$$

$$f^{0}(r) = 1/2[f^{+}(r) + f^{-}(r)] \quad \text{(for radial attack)}$$

In a finite difference approximation, the condensed Fukui function[29] of an atom, say x, in a molecule with N electrons is defined as

$$f_x^{+} = [q_x(N+1) - q_x(N)] \quad \text{(for nucleophilic attack)} \quad (2)$$

$$f_x^{-} = [q_x(N) - q_x(N-1)] \quad \text{(for electrophilic attack)}$$

$$f_x^{0} = [q_x(N+1) - q_x(N-1)]/2 \quad \text{(for radical attack)}$$

where q_x is the electronic population of atom x in a molecule. In DFT, hardness (η) is defined as[30]

$$\eta = 1/2(\delta^2 E/\delta N^2)\, v(r) = 1/2(\delta\mu/\mathrm{d}N)_v$$

The global softness, S, is defined as the inverse of the global hardness, η:

$$S = 1/2\eta = (\delta N/\delta\mu)_v$$

The local softness $s(r)$ can be defined as

$$s(r) = (\delta\rho(r)/\delta\mu)_v \quad (3)$$

Equation 3 can also be written as

$$s(r) = [\delta\rho(r)/\delta N]_v\,[\delta N/\delta\mu]_v = f(r)S \quad (4)$$

Thus, local softness contains the same information as the Fukui function $f(r)$ plus additional information about the total molecular softness, which is related to the global reactivity with respect to a reaction partner, as stated in the HSAB principle. Using the finite difference approximation, S can be approximated as

$$S = 1/(\mathrm{IE} - \mathrm{EA}) \quad (5)$$

where IE and EA are the first ionization energy and electron

affinity of the molecule, respectively. Atomic softness values can easily be calculated by using eq 4, namely

$$s_x^+ = [q_x(N+1) - q_x(N)]S \tag{6}$$

$$s_x^- = [q_x(N) - q_x(N-1)]S$$

$$s_x^0 = S[q_x(N+1) - q_x(N-1)]/2$$

Definition of λ. The interaction energy between two chemical species A and B with the number of electrons N_A and N_B can be written within the framework of DFT as

$$\Delta E_{inter} = E[\rho_{AB}] - E[\rho_A] - E[\rho_B] \tag{7}$$

where, ρ_{AB}, ρ_A, and ρ_B are the electron densities of the systems AB at equilibrium and of the isolated systems A and B, respectively. Now, from the proposition of Gazquez and Mendez,[31] when A and B interact, they can be interacted in two steps: (1) interaction will take place through the equalization of chemical potential at constant external potential and (2) A and B approach the equilibrium state through changes in the electron density of global system generated by making changes in the external potential at constant chemical potential. Thus, the total interaction energy between A and B becomes[31]

$$\Delta E_{inter} = \Delta E_v + \Delta E_\mu \tag{8}$$

where

$$\Delta E_\nu = -1/2[(\mu_A - \mu_B)^2/(S_A + S_B)](S_A S_B)$$

$$\Delta E_\mu = -1/2 N_{AB}{}^2 k[1/(S_A + S_B)]$$

where N_{AB} is the total number of electrons of the system AB and k is proportionality constant between S_{AB} and $S_A + S_B$. The product of N^2 and k is known as λ:

$$\Delta E_\mu = -(1/2)\lambda/(S_A + S_B)$$

Hence, λ[32,33] is related to the effective number of valence electrons that participate in the interaction between A and B.

Now, applying the proposition of Pal et al.,[28] from a local point of view, if the interaction between two chemical systems A and B occurs through the jth atom of A, then the interaction at the jth atom of A can be expressed by replacing the global softness of A with the local softness of the site j in A. Then λ can be defined as the change in electron densities of the system before and after the interaction process. Now, if the change in the electron density of a system A is only at the site of interaction j of A, then λ can be effectively the change of electron density at the site j:

$$\lambda_{Aj} = q_{Aj}^{eq} - q_{Aj}^0 \tag{9}$$

where q_{Aj}^{eq} and q_{Aj}^0 are the densities of the jth atom of the system A in the complex AB and in the isolated system A, respectively.

The approximation here is that the interaction takes place through one atom of the interacting molecule. The environment of the interacting atom site is not considered.

Computational Methodology and Model

In the present study, all calculations have been carried out with DFT[34] using DMOL code of MSI Inc. BLYP[35,36] exchange correlation functional and DNP basis set[37] were used throughout the calculation. BLYP has already shown its credibility for explaining weak hydrogen bond type interactions in comparison to MP2 level calculations.[38,39] It is also useful in describing the interaction of heteroatomic molecules with zeolite framework cluster.[23a] Basis set superposition error (BSSE) was also calculated for the current basis set in nonlocal density approximation (NLDA) using the Boys−Bernardi method.[40] Geometries of the interacting nitrogen heterocyclics pyrrole, indole, pyridine, and imidazole along with the individual clay cluster models representing different isomorphous substitution in the octahedral aluminum of dioctahedral smectites were fully optimized for calculating the reactivity index. The detailed theory for calculating reactivity index is mentioned in our earlier article as well as in other articles.[23] Single-point calculations of the cation and anion of each molecule at the optimized geometry of the neutral molecule were also carried out to evaluate Fukui functions and global and local softness. The condensed Fukui function and atomic softness were evaluated using eqs 2 and 6, respectively. The gross atomic charges were evaluated by using the technique of electrostatic potential (ESP) driven charges. It is well-known that Mulliken charges are highly basis set dependent, whereas ESP driven charges show less basis set dependence[23,41,42] and are better descriptors of the molecular electronic density distribution.

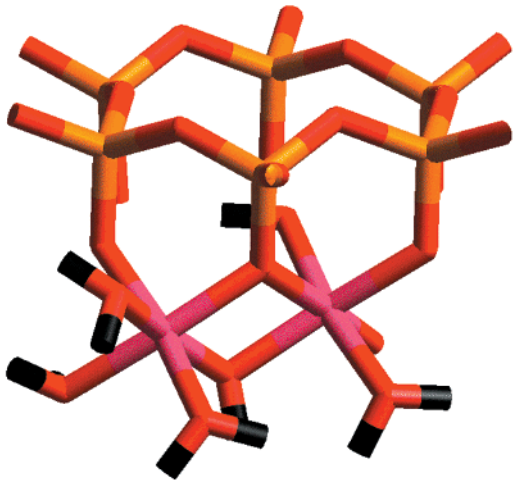

Figure 1. Cluster model of montmorillonite with six tetrahedral silicons and two octahedral aluminums. It is the top view of the cluster. The color code is as follows: red (oxygen); yellow (silicon); violet (octahedral aluminum); black (hydrogen).

The ideal formula of the clay montmorillonite, a member of 2:1 dioctahedral smectite family, is $(Na_x^+, nH_2O)(Al_{4-x}Mg_x)Si_8O_{20}(OH)_4$.[43] The $Al_2Si_6O_{24}H_{18}$ cluster was generated from the clay structure as shown in Figure 1. Figure 1 displays the top view of one tetrahedral and one octahedral sheet, showing the hexagonal cavities at the oxygen surface of the silicon layers. The dangling bonds were saturated with hydrogens, not shown in Figure 1 for visual clarity. The hydroxyl group at the center of the hexagonal cavity is parallel to the clay surface and pointing in the direction of the vacancy of the octahedral network. Of the two octahedral aluminums, one is more stable than the other, as reported in our earlier study.[43] Therefore, to mimic the isomorphous substitution, calculations were performed on a cluster model with formula $TSi_4O_{16}H_{10}$, where T = Fe^{3+}, Mg^{2+}, Fe^{2+}, or Li^+, where the adjacent silicon and aluminum atoms occurring in the clay lattice are replaced by hydrogens to preserve the electroneutrality of the model as shown in Figure 2. The substitution energy was calculated for

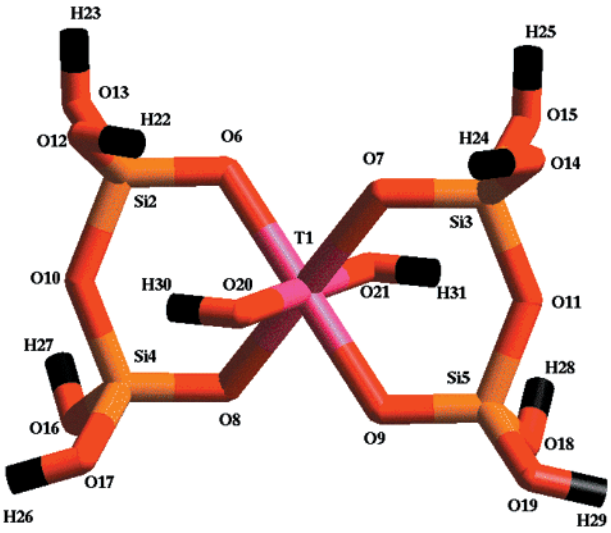

Figure 2. Initial configuration of a clay cluster having the formula $TSi_4O_{16}H_{10}$. All of the atoms are labeled as shown in Table 3. The color code is as follows: red (oxygen); yellow (silicon); violet (octahedral aluminum); black (hydrogen).

TABLE 1: Nonlocal Density Functional Study of $AlSi_4O_{16}H_{10}$ Cluster to Calculate the Substitution Energy for Different Substituent in Place of Octahedral Al^{3+}

substituent metal ion	substituted cluster	substitution energy (eV)
Li^+	$[LiSi_4O_{16}H_{10}]^{2-}$	−12.59
Mg^{2+}	$[MgSi_4O_{16}H_{10}]^-$	−12.75
Fe^{2+}	$[FeSi_4O_{16}H_{10}]^-$	−12.68
Fe^{3+}	$[FeSi_4O_{16}H_{10}]$	−12.86

TABLE 2: Global Softness Values (in au) for Clay Clusters $[AlSi_4O_{16}H_{10}]$ with Different Isomorphously Substituted Octahedral Cations (in Place of Al^{3+}) and Nitrogen Heterocyclic Molecules

molecules	global softness (au)
$[LiSi_4O_{16}H_{10}]^{2-}$	1.862
$[MgSi_4O_{16}H_{10}]^-$	1.521
$[FeSi_4O_{16}H_{10}]^-$	1.467
$[FeSi_4O_{16}H_{10}]$	1.288
pyrrole	2.625
pyridine	2.574
indole	2.874
imidazole	2.098

the most active aluminum between the two by the following equation as mentioned in our earlier study:[44]

$$AlSi_4O_{16}H_{10} + TO_4^- \rightarrow TSi_4O_{16}H_{10} + AlO_4^-$$

Results and Discussion

The electronic and structural properties of nitrogen heterocyclics along with the clay cluster models are first rationalized. The substitution energies calculated for the clay cluster models are presented in Table 1. The global softness values of the clay cluster models as well as the interacting molecules are calculated using DFT and are presented in Table 2. The values of nucleophilic condensed local softness (s_x^+) and condensed Fukui function (f_x^+) of the individual atoms of the clay cluster models obtained through ESP technique at DFT level are shown in Table 3. The effect of H−O−T angles for the clay clusters were measured, where T = Fe^{3+}, Mg^{2+}, Fe^{2+}, or Li^+. The results are shown in Table 4. The values of electrophilic condensed

TABLE 3: Condensed Local Softness and Fukui Function Values (au) for Clay Clusters with Different Isomorphous Substitution by ESP Technique Using DFT

	substituent cation for octahedral Al^{3+}							
	Mg^{2+}		Fe^{3+}		Fe^{2+}		Li^+	
atoms	f_x^+	s_x^+	f_x^+	s_x^+	f_x^+	s_x^+	f_x^+	s_x^+
T1	0.150	0.229	0.221	0.284	0.144	0.212	0.097	0.180
Si2	0.058	0.089	0.093	0.120	0.049	0.073	0.040	0.074
Si3	0.060	0.092	0.088	0.113	0.051	0.075	0.045	0.083
Si4	0.063	0.097	0.098	0.126	0.053	0.079	0.046	0.085
Si5	0.053	0.082	0.076	0.098	0.048	0.071	0.044	0.081
O6	0.054	0.083	0.059	0.076	0.051	0.075	0.043	0.080
O7	0.060	0.092	0.072	0.093	0.059	0.087	0.045	0.083
O8	0.064	0.098	0.065	0.084	0.055	0.082	0.043	0.080
O9	0.063	0.097	0.104	0.134	0.055	0.081	0.042	0.078
O10	0.061	0.093	0.087	0.112	0.055	0.081	0.041	0.076
O11	0.051	0.078	0.093	0.119	0.056	0.083	0.044	0.081
O12	0.052	0.079	0.069	0.088	0.060	0.089	0.040	0.074
O13	0.053	0.081	0.097	0.125	0.057	0.084	0.041	0.076
O14	0.057	0.087	0.084	0.108	0.050	0.074	0.042	0.078
O15	0.054	0.083	0.123	0.159	0.053	0.079	0.046	0.085
O16	0.064	0.098	0.078	0.100	0.057	0.085	0.040	0.074
O17	0.061	0.093	0.106	0.136	0.059	0.087	0.041	0.076
O18	0.052	0.079	0.079	0.101	0.049	0.072	0.044	0.081
O19	0.047	0.073	0.055	0.070	0.053	0.078	0.040	0.074
O20	**0.402**	**0.612**	**0.275**	**0.354**	**0.325**	**0.478**	**0.124**	**0.231**
O21	**0.458**	**0.698**	**0.348**	**0.448**	**0.370**	**0.543**	**0.149**	**0.277**
H22	0.016	0.025	0.015	0.019	0.012	0.018	0.010	0.018
H23	0.012	0.019	0.010	0.013	0.013	0.020	0.010	0.018
H24	0.013	0.021	0.017	0.021	0.014	0.021	0.011	0.020
H25	0.015	0.024	0.012	0.015	0.015	0.023	0.012	0.021
H26	0.013	0.021	0.011	0.014	0.012	0.019	0.011	0.020
H27	0.013	0.020	0.014	0.018	0.012	0.019	0.012	0.021
H28	0.011	0.018	0.018	0.023	0.013	0.020	0.011	0.020
H29	0.011	0.018	0.017	0.021	0.012	0.019	0.010	0.018
H30	**0.323**	**0.492**	**0.335**	**0.432**	**0.314**	**0.462**	**0.211**	**0.393**
H31	**0.396**	**0.603**	**0.428**	**0.551**	**0.400**	**0.587**	**0.233**	**0.434**

TABLE 4: H−O−T Bond Angles for Clay Cluster Models with Different Isomorphous Substituent Cation

clay cluster	H−O−T
$[LiSi_4O_{16}H_{10}]^{2-}$	90.78
$[MgSi_4O_{16}H_{10}]^-$	102.78
$[FeSi_4O_{16}H_{10}]^-$	102.21
$[FeSi_4O_{16}H_{10}]$	101.97

TABLE 5: Condensed Local Softness and Fukui Function Values (in au) for Nitrogen Heterocyclics Using ESP Technique with DFT

	ESP technique	
atoms of interacting molecules	f_x^-	s_x^-
N of imidazole	0.523	1.097
N of pyridine	0.423	1.088
N of indole (−NH)	0.101	0.298
N of pyrrole (−NH)	0.122	0.317

local softness (s_x^-) and condensed Fukui function (f_x^-) of the individual atoms of the interacting individual molecules obtained through ESP technique at DFT level are shown in Table 5. It is observed from Table 2 that those global softness values for the clay cluster models are lower than that of the interacting molecular species. So, to test the HSAB principle, it seems to be important to analyze whether the local softness values, Fukui functions, or reactive indices for the constituent atoms of the cluster models and interacting molecular species will be a more reliable parameter. First, the interaction of all of the clay cluster models containing different isomorphous substituent cations with individual nitrogen heterocyclic molecules is calculated using local softness values, and an activity order is proposed. This order is validated by the interaction energy calculations. The

new parameter λ has also been calculated, and quantitative information has been generated from the results that are shown in Table 7. The orientation of the optimized interacting molecule conformation is also monitored to justify its interaction with hydroxyl hydrogen attached with octahedral alumina of the clay framework.

A. Structure, Electronic Properties, and Reactivity Index of the Isomorphously Substituted Clay Cluster. Isomorphous substitution of an Al^{3+} ion at an octahedral site by Li^+, Mg^{2+}, Fe^{2+}, and Fe^{3+} was studied. In each case, the cluster was totally optimized. The initial configuration with labeled atoms of one of the clusters is shown in Figure 2. The variation of the orientation and other geometric parameters of the hydroxyl hydrogen attached to the octahedral site were monitored. As we have seen earlier, there are two different aluminum present in the dioctahedral smectites with different geometric parameters.[44] The substitution energy was calculated for the most active aluminum between the two, by the equation mentioned in the theory section. The substitution energy shows that the preference is in iron (Fe^{3+}). The order of substitution follows the order $Fe^{3+} > Mg^{2+} > Fe^{2+} > Li^+$. It is noted below that the magnitude of electron density (numbers in parentheses) transferred to the metal ion is Al^{3+} (2.56) > Fe^{3+} (2.09) > Mg^{2+} (1.52) > Fe^{2+} (1.28) > Li^+ (0.06). Thus, rather than the formal charges associated with the various cations, the calculated in situ net charges are given by 0.44+, 0.91+, 0.48+, 0.72+, and 0.94+, where the same cation order as in above set of inequalities has been kept. This ordering agrees with the proposal of Goldschmidt.[45] His proposal was based on the approximate relative sizes of metal ions in their appropriate valences. The results partially are in agreement with the stability order proposed by Arnowitz et al. for isomorphous substitution clays using self-consistent charge extended Huckel program.[46] It is observed that insertion of Li^+ in place of Al^{3+} in the octahedral layer is the least favorable process.

Now as we have mentioned in our earlier paper,[43] the orientation of hydroxyl hydrogen attached to the octahedral aluminum or the isomorphously substituted cation plays a crucial role in its acidity and activity. Hence, we calculated the Fukui function (f_x^+) and local atomic softness (s_x^+) for the constituent atoms of the isomorphously substituted clusters by ESP charges obtained from DFT and tabulated the results in Table 3. The results show that the activity order is different from that of the order predicted by the substitution energy. The substitution energy results predicted that Fe^{3+} substitution incur most stability, but when we try to monitor the activity of the hydroxyl group attached to the octahedral cation, we get a different scenario. In a situation with Mg^{2+} as the isomorphous substituent, the hydroxyl hydrogen shows most nucleophilicity as shown in Table 3. In terms of activity of the hydroxyl group, the order stands $Mg^{2+} > Fe^{2+} > Fe^{3+} > Li^+$. To resolve the ambiguity, we calculated the geometric parameters for the all optimized structures of isomorphously substituted clusters, and an explanation is generated. It is observed that the geometry of the active site is affected with the nature of cation present in the octahedral site substituting aluminum. The variation of H−O−T angle for each substituted situation is tabulated in Table 4. The result shows the activity order as predicted from Fukui function are explainable. We monitored the H−O−T angle to account for the activity of the hydroxyl hydrogen attached with the octahedral cation, as the activity of the hydroxyl hydrogen is dependent on its environment and orientation. This means that the availability of the hydroxyl hydrogen attached to the octahedral magnesium is the maximum, or in other words the hydroxyl hydrogen will be the most active in case of magnesium substitution in comparison to other isomorphic substituents. The substitution energy order shows that in the case of Fe^{3+} the structure gets most stabilized energetically which may be due to many other reasons as shown in our earlier study.[44] However, for the situation with the sorbent, the interacting molecule will be attracted by a moiety of active interaction favoring the sorption process. The interacting molecule then should pave its way through the hexagonal hole resulting from the six silicon on the clay surface and will approach to the most nucleophilic site of the clay surface, or in other words, the most electrophilic site of the nitrogen heterocyclics will interact with most nucleophilic site of clay surface, assuming that none of the tetrahedral silicon present on the clay surface layer is substituted by tetrahedral aluminum to generate some surface acidity. The aim is to find a match for the nucleophilic center present in the magnesium substituted clay cluster and the electrophilic site of the interacting nitrogen heterocyclic molecules. The specific interaction of the molecule with clay surface will be discussed in the following sections.

B. Interaction of Isomorphously Substituted Clay Clusters with Nitrogen Heterocyclic Molecules. We have chosen four different nitrogen heterocyclic molecules, namely, pyrrole, indole, imidazole, and pyridine. Table 5 presents the condensed local softness and Fukui functions for the most electrophilic site of the interacting molecules. The results show that for all of the cases the most electrophilic site is the nitrogen atom single or bonded as −NH. Now these active centers will interact with the most nucleophilic site of the clay clusters, which is the bridging hydroxyl, attached with octahedral cation present. It is observed from the Fukui functions or condensed local softness values that, among the four molecules, there may exist two sets of molecules in terms of the close values of local softness. One set consists of imidazole and pyridine, and the other consists of indole and pyrrole. Now the groups have one thing in common, i.e., the active center. For the first group, it is N, and for the second set, it is also N but from the −NH moiety. This provokes us to try two types of adsorption complex, one is through N and the other is through −NH, which may help us to investigate two different complex formation processes (1) through the hydrogen bonding and (2) through the cation−π interaction. This can be achieved by performing interaction between these two sets of molecules with most active clay cluster in terms of the activity. If the interaction energy follows the same trend, then we can say that Fukui Functions can comprehensively propose the intermolecular level interactions.

C. Reactivity Index Scale. It is observed that all of the nitrogen heterocyclic molecules have a higher global softness value in comparison to interacting clay clusters with different isomorphous substitution. The order of global softness of different isomorphously substituted clay clusters irrespective of nitrogen heterocyclics is as follows:

$$Li^+ > Mg^{2+} > Fe^{2+} > Fe^{3+}$$

whereas that for the nitrogen heterocyclics is

$$\text{indole} > \text{pyrrole} > \text{pyridine} > \text{imidazole}$$

The results show that both in terms of Fukui functions and condensed local softness the hydroxyl hydrogen attached to different octahedral cation through oxygen bridge in interacting clay cluster can be arranged in the order $Mg^{2+} > Fe^{2+} > Fe^{3+} > Li^+$. Here we propose a scale of activity of clay material of 2:1 smectite family having isomorphous substituent in the

TABLE 6: Comparison of Local Softness of the Electrophilic Center of Nitrogen Heterocyclics and Nucleophilic Center of Clay Cluster s_x^+/s_x^- (au)

nucleophilic atom centers of clay cluster with	s_x^+/s_x^- interacting nitrogen heterocyclics with electrophilic N center			
	imidazole	pyridine	indole	pyrrole
	Mg^{2+}			
(a)H30	0.451	0.455	1.696	1.587
(b)H31	0.553	0.558	2.079	1.945
	Fe^{2+}			
(a)H30	0.423	0.427	1.593	1.490
(b)H31	0.538	0.543	2.024	1.893
	Fe^{3+}			
(a)H30	0.396	0.400	1.593	1.490
(b)H31	0.505	0.510	2.024	1.893
	Li^+			
(a)H30	0.360	0.363	1.355	1.267
(b)H31	0.398	0.401	1.496	1.400

octahedral cation position to locate the most active material for nitrogen heterocyclics sorption. Now we compared the condensed local softness and Fukui functions of the most electrophilic atom of the individual nitrogen heterocyclic. The results show that the activity of nitrogen heterocyclics is as follows:

imidazole > pyridine > pyrrole > indole

The local softness of imidazole and pyridine are higher than the rest. This is may be due to the presence of lone pair in their respective structures.

D. Interaction of Nitrogen Heterocyclic Molecules with the Clay Cluster Model: A Quantitative Analysis. We first compared the local softness values of the nucleophilic center with different isomorphous substitution with the electrophilic center present in nitrogen heterocyclics to choose the best candidate for the sorption. The results are shown in Table 6. The result in terms of s_x^+/s_x^- show that hydroxyl hydrogen attached to the cluster with Mg^{2+} substituent is the best for interacting nitrogen heterocyclics in general. This idea has been proposed by Roy et al.[47] to predict intramolecular and intermolecular reactivity sequences of carbonyl compounds. Now this ratio of local softness parameters behaves nicely for intramolecular interaction, but for intermolecular interaction, this methodology is purely qualitative in nature. The trend matches the experimental activity order. The order of activity is in the order imidazole > pyridine > pyrrole > indole. The little higher value of pyrrole and indole makes us believe that apart from the proposed weak interaction between interacting atoms of a molecule there may exist some other interactions, which may be of the cation$-\pi$ type. The clay clusters (Mg^{2+} substituent) at their respective optimized structures were fixed, and heterocyclic molecules are optimized. For each case, the most electrophilic atom (as observed from the reactive index values) of the interacting molecule was placed at a distance of 2.5 Å from the hydroxyl hydrogen attached to the octahedral cation of clay cluster acting as the nucleophilic center. Now, from the results of Table 6, we decided to choose two initial configurations for the interaction (1) through the atom with a lone pair of electrons resulting in a hydrogen bonded complex and (2) through the ring then the cation$-\pi$ complex is the most feasible one as supported by the study with ammonium cation by Zhu et al.[8] The minimum energy conformer comes from the optimization starting with the first configuration. In the optimized structure, it is easily recognized that the heterocyclic

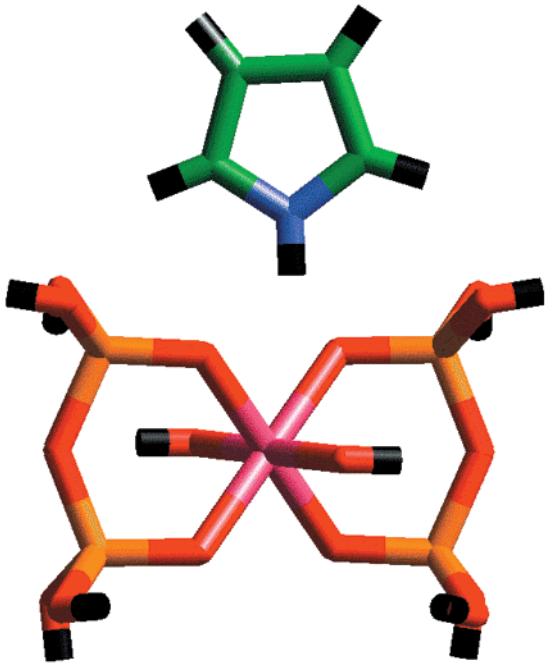

Figure 3. Structure of pyrrole molecule at its initial configuration during interaction with clay cluster. The color code is as follows: red (oxygen); green (carbon); indigo (nitrogen); black (hydrogen).

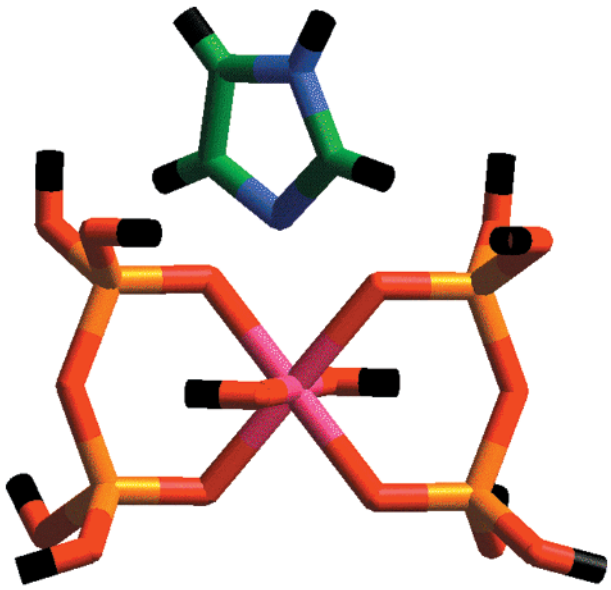

Figure 4. Structure of imidazole molecule at its initial configuration during interaction with clay cluster. The color code is as follows: red (oxygen); green (carbon); indigo (nitrogen); black (hydrogen).

molecule moves closer to the nucleophilic site and the distance between the nucleophilic and electrophilic atom varies with the affinity. The orientations of the pyrrole and imidazole molecules with respect to the clay cluster are shown in Figures 3 and 4, respectively. The results of the total energy of the individual framework clusters and the interacting molecules along with the adsorption complex and the interaction energy (BSSE corrected) of the cases are shown in Table 7. The interaction energy values fall in the range of 11.63−15.20 kcal/mol. We will not emphasize on the numbers; rather, we will analyze the trend. The interaction energy values show the order with respect to the sorption of heterocyclics:

imidazole > pyridine > pyrrole > indole

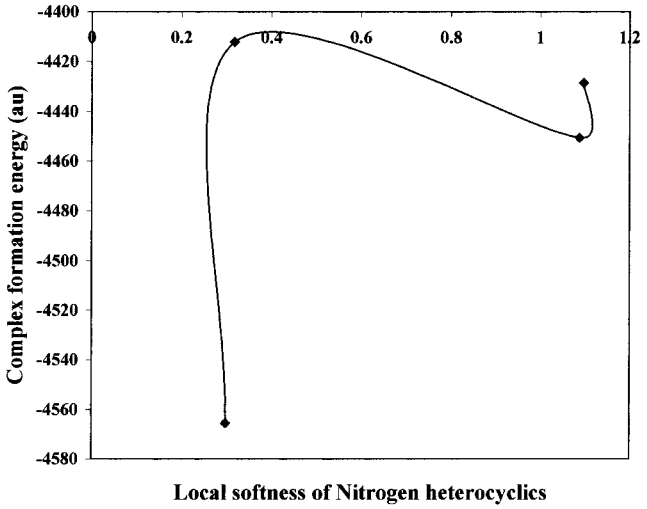

Figure 5. Complex formation energy with respect to the local softness values for the electrophilic center of the nitrogen heterocyclic molecules.

TABLE 7: Total Energy of the Framework Cluster and Interacting Molecules along with Interaction Energy (BSSE Corrected) Followed by Evaluation of λ

molecule	total energy (au)	interaction energy (kcal/mol) BSSE corrected	λ (au)
framework	−4202.0752		
pyrrole	−210.1378		
pyridine	−248.2527		
indole	−363.7634		
imidazole	−226.4054		
FW + pyrrole	−4412.2350	−13.82	0.054
FW + pyridine	−4450.3518	−15.02	0.082
FW + indole	−4565.8571	−11.63	0.032
FW + imidazole	−4428.5048	−15.20	0.115

Though the results are qualitative, they match with the order predicted in terms of reactivity index values. The results also show that for the interactions through nitrogen results in a stronger adsorption complex in comparison to the other set where the interaction is through the −NH center. The geometrical parameters calculated from the optimized geometry show that the molecules with a lone pair of electrons move closer to the active center of the clay cluster in comparison to the other set. Whereas for the other set, the distance between the ring and the proton center decreases, the distance between the −NH and the hydroxyl hydrogen remains unchanged. This validates the proposition of Zhu et al.,[8] which suggests that imidazole or pyridine has a N atom with localized lone pair of electrons that has the ability to form a H-bond type interaction with the hydroxyl hydrogen present in clay. Whereas, the heteroatoms in pyrrole and indole have almost no such affinity for the hydroxyl hydrogen as observed from the results shown in Table 6, their electrons are delocalized. Hence, for the first pair, the interaction may be of H-bonding type, and for the second set, it may be of the cation−π type. Complex formation energy has been plotted with respect to the local softness of the nucleophilic center of nitrogen heterocyclics and is shown in Figure 5. The results show that the complex formation energy decreases with an increase in the softness value. The greater the softness value, the less negative the complex formation energy is. The plot also shows that molecules with higher softness values fall in close range in terms of formation energy, whereas molecules with lower softness have a marked difference in complex formation energy. The difference in formation energy between pyrrole and indole is due to their structural dissimilarities. Now to resolve the issue quantitatively, we have chosen the following procedure. With the help of the new λ parameter, one can give a quantitative estimate for weak interactions with a consideration that the interaction is a unisite one. As we predicted earlier, the reactivity index scale is valid for a unit site interaction. The study has been supported by the results obtained for zeolites.[20] Gazquez et al.[48] as well as Mendez[49] et al. have used approximate values of λ to describe the reactivity of enolate ions and 1,3-cycloaddition reactions of benzonitrile oxide with an alkene, respectively. The approximate values may be enough for their explanation, but the bonding involved here is quite different from the bonding situation of theirs. Now in our case, there exists a weak interaction between the heterocyclic molecules with the clay framework, either through the H-bonding or through the cation−π interaction. Now while deriving λ, we assume that when organic molecule and clay clusters are interacting weakly through the nitrogen atom of the organic molecule and the hydrogen atom of the clay cluster only these two atoms of organic and clay clusters are involved in the interaction. The involvement of neighbors is neglected. Hence, the greatest change in population will only occur at the atomic sites of the interacting molecule. The values of λ are shown in Table 6 as well as calculated using eq 9. It is observed that all of the λ values are small and positive. The λ value is maximum for imidazole, and the trend is imidazole > pyridine > pyrrole > indole. The lower values of λ for pyrrole and indole indicate which may result due to cation−π interaction, but λ is unable to account for it. The results show that the prediction holds good for unisite interaction. This also validates our earlier proposition[26] that the reactivity index scale is nice for unit site interaction. The results clearly identify the existence of two types of interactions. As it is observed, pyrrole and indole fall in one group, whereas pyridine and imidazole form the other. The differences in values of the interaction energies were of few kcals, which though shows the trend qualitatively, but one cannot conclusively defend the result. However, with the new parameter λ, one can quantitatively defend the numbers and hence the activities. This is undoubtedly a new finding, and it also validates our earlier proposition that with unisite interaction the reactivity index scale works nicely. The optimistic results pave the way of generating models for multisite interaction. This methodology can now be extrapolated to other materials and typical reactions, which saves tedious experimentation.

Conclusion

This is the first study to rationalize the activity of dioctahedral clays on the adsorption of nitrogen heterocyclics mimicking large biomolecules using local reactivity descriptors. A new parameter was introduced for the first time, λ, which shows to be a quantitative descriptor of interatomic interaction taking place between interacting molecules in the helm of DFT. We successfully identified the best cation present in dioctahedral clays which can act as a best sorbent for nitrogen heterocyclics. At the same time, we could identify two different kinds of interaction occurring between the nitrogen heterocyclics. It has also been possible to locate the groups of molecules for which the hydrogen bonding type interaction is the most favorable one (pyrrole and indole) and the other group for which the cation−π interaction is the most feasible one (pyridine and imidazole). This study also validates our earlier proposition regarding unisite interaction.

References and Notes

(1) Ma, J. C.; Dougherty, D. A *Chem. Rev.* **1997**, *97*, 1303.
(2) Basch, H.; Stevens, W. J. *J. Mol. Struct. (THEOCHEM)* **1995**, *338*, 303.
(3) Deakyne, C. A.; Meot-Ner, M. *J. Am. Chem. Soc.* **1985**, *107*, 474.
(4) Mo, O.; Yanez, M.; Elguero, J. *J. Org. Chem.* **1987**, *52*, 1713.
(5) Petti, M. A.; Shepodd, T. J.; Barrans, J. R. E.; Dougherty, D. A. *J. Am. Chem. Soc.* **1988**, *110*, 6825.
(6) Matyus, P.; Fuji, K.; Tanak, K. *Tetrahedron* **1994**, *50*, 1405.
(7) Tan, X. J.; Jiang, H. L.; Chen, K. X.; Ji, R. Y. *J. Chem. Soc., Perkin Trans. 2* **1999**, 107.
(8) Zhu, W. L.; Jiang, H. L.; Puah, C. M.; Tan, X. J.; Chen, K. X.; Cai, Y.; Ji, R. Y. *J. Chem. Soc., Perkin Trans. 2* **1999**, 2615.
(9) Lee, J. F.; Mortland, M. M.; Chiou, C. T.; Kile, D. E.; Boyd, S. A. *Clays Clay Minerals* **1990**, *38*, 113.
(10) Chiou, C. T.; Kile, D. E.; Malcolm, R. L. *Environ. Sci. Technol.* **1988**, *22*, 298.
(11) Chiou, C. T.; Shoup, T. D. *Environ. Sci. Technol.* **1985**, *19*, 1196.
(12) Bailey, S. W. *Am. Mineral.* **1975**, *60*, 175.
(13) Sposito, G.; Prost, R. *Chem. Rev.* **1982**, *82*, 553.
(14) Delville, A. *Langmuir* **1991**, *7*, 547.
(15) Giese, R. F. *Nature* **1973**, *241*, 151.
(16) Pearson, R. G. *J. Am. Chem. Soc.* **1983**, *105*, 7512.
(17) Pearson, R. G. *J. Chem. Educ.* **1987**, *64*, 561.
(18) Parr, R. G.; Yang, W. *J. Am. Chem. Soc.* **1984**, *106*, 4049.
(19) Langenaeker, W.; Demel, K.; Geerlings, P. *J. Mol. Struct. (THEOCHEM)* **1992**, *259*, 317.
(20) Langenaeker, W.; De Proft, F.; Geerlings, P. *J. Phys. Chem.* **1995**, *99*, 6624.
(21) Langenaeker, W.; De Proft, F.; Geerlings, P. *J. Phys. Chem. A* **1998**, *102*, 5944.
(22) Chandra, A. K.; Geerlings, P.; Nguyen, M. T. *J. Org. Chem.* **1997**, *62*, 6419.
(23) (a) Chatterjee, A.; Iwasaki, T.; Ebina, T. *J. Phys. Chem. A* **1999**, *103*, 2489 and references therein. (b) Chermette, H. *J. Comput. Chem.* **1999**, *20*, 129. (c) Geerlings, P.; De Proft, F.; Langenaeker, W. *Adv. Quantum Chem.* **1999**, *33*, 103.
(24) Gazquez, J. L.; Mendez, F. *J. Phys. Chem.* **1994**, *98*, 4591.
(25) Chatterjee, A.; Iwasaki, T. *J. Phys. Chem. A* **1999**, *103*, 9857.
(26) Chatterjee, A.; Iwasaki, T.; Ebina, T. *J. Phys. Chem. A* **2000**, *104*, 2098.
(27) Chatterjee, A.; Iwasaki, T.; Ebina, T. *J. Phys. Chem. A* **2000**, *104*, 8216.
(28) Pal, S.; Chandrakumar, K. R. S. *J. Am. Chem. Soc.* **2000**, *122*, 4145.
(29) Yang, W.; Mortier, M. J. *J. Am. Chem. Soc.* **1986**, *108*, 5708.
(30) Pearson, R. G.; Parr, R. G. *J. Am. Chem. Soc.* **1983**, *105*, 7512.
(31) Gazquez, J. L.; Mendez, F. *J. Am. Chem. Soc.* **1994**, *116*, 9299.
(32) Parr, R. G.; Gazquez, J. L *J. Phys. Chem.* **1993**, *97*, 3939.
(33) Gazquez, J. L. *Struct. Bonding* **1993**, *80*, 27.
(34) Kohn, W.; Sham, L. J. *Phys. Rev. A* **1965**, *140*, 1133.
(35) Becke, A. *J. Chem. Phys.* **1988**, *88*, 2547.
(36) Lee, C.; Yang, W.; Parr, R. G. *Phys. Rev. B* **1988**, *37*, 786.
(37) Bock, C. W.; Trachtman, M. *J. Phys. Chem.* **1994**, *98*, 95.
(38) (a) Sim, F.; St-Amant, A.; Papai, I.; Salahub, D. R. *J. Am. Chem. Soc.* **1992**, *114*, 4391. (b) Kim, K.; Jordan, K. D. *J. Phys. Chem.* **1994**, *98*, 10089.
(39) Chandra, A. K.; Nguyen, M. T. *Chem. Phys.* **1998**, *232*, 299.
(40) Boys, S. F.; Bernardi, F. *Mol. Phys.* **1970**, *19*, 553.
(41) De Proft, F.; Martin, J. M. L.; Geerlings, P. *Chem. Phys. Lett.* **1996**, *250*, 393.
(42) Geerlings, P.; De Proft, F.; Martin, J. M. L. Recent Developments in Density Functional Theory. In *Theoretical and Computational Chemistry 5*; Seminario, S., Ed.; Elsevier: Amsterdam, 1996; pp 773−780.
(43) Chatterjee, A.; Hayashi, H.; Iwasaki, T.; Ebina, T.; Torii, K. *J. Mol. Catal. A* **1998**, *136*, 195.
(44) Chatterjee, A.; Iwasaki, T.; Ebina, T.; Hayashi, H. *J. Mol. Graphics* **1996**, *14*, 302.
(45) Goldschmidt, V. M. *Skr. Nor. Vidensk Akad. [Kl.], Mat. Naturvidensk. Kl.* **1926**.
(46) Arnowitz, S.; Coyne, L.; Lawless, J.; Rishpon, J. *Inorg. Chem.* **1982**, *21*, 3589.
(47) Roy, R. K.; Krishnamurti, S.; Geerlings, P.; Pal, S. *J. Phys. Chem. A* **1998**, *102*, 3746.
(48) Gazquez, J. L.; Mendez, F. *Proc. Ind. Acad. Sci.* **1994**, *106*, 183.
(49) Mendez, F.; Tamariz, J.; Geerlings, P. *J. Phys. Chem. A* **1998**, *102*, 6292.